3D Mesh Wavelet Coding Using Efficient Model-based Bit Allocation *

Frédéric PAYAN, Marc ANTONINI
I3S laboratory, CNRS and University of Nice-Sophia Antipolis
2000, route des lucioles, 06903 Sophia-Antipolis, France
E-mail: fpayan@i3s.unice.fr, am@i3s.unice.fr

Abstract

In this paper, we propose an efficient low complexity geometry compression scheme for densely sampled irregular 3D meshes. This scheme is based on 3D multiresolution analysis (3D Discrete Wavelet Transform) and includes a model-based bit allocation process across the wavelet subbands. Coordinates of 3D wavelet coefficients are processed separately and statistically modeled by a generalized Gaussian distribution. This permits an efficient allocation even at low bitrate with very low complexity. Moreover, we introduce predictive geometry coding of LF subbands by taking in account the correlation of the coarsest level coefficients. Finally, we use EBCOT coder to efficiently encode the quantized coefficients.

1 Introduction

Triangular meshes are a powerfool tool for modeling the shape of complex 3D objects. Because of their simplicity (points and edges), they are easily manipulated and more and more present in 3D models visualisation setting. Triangular meshes, resulting from 3D acquisition techniques, are finely detailled and highly sampled. Unfortunately they are very complex (irregular connectivity) and have tremendous size. Hence, they are awkward for computation, storage or transmission. The goal of compression algorithms is to strongly reduce the quantity of data to represent an object for a given global quality. In 2D image compression, the tools are well developed since decades and algorithms are now very efficient [12]. However, compression of 3D meshes are relatively new. Generally, they involve geometry and topology data compression, and the performances of these kind of methods can be found in [10]. Our framework is based on multiresolution analysis theory like in [3, 5] and rate/distortion theory instead of a non progressive compression like [2, 9]. This paper is organized as follow. Section 2 introduces the global compression scheme. Section 3 exposes the statistical distribution of the wavelet coefficients used for the model-based bit allocation developed in section 4. Finally, we present simulation results and compare our algorithm with the PGC method in section 5 and conclude in section 6.

2 Proposed geometry coder

The first step of our geometry compression scheme (see figure 1) is to obtain a semi-regular mesh of the original irregular mesh. The technique used is MAPS [4]. Hence, a Discrete Wavelet Transform (DWT) can be applied on the semi-regular mesh to obtain a multiresolution representation: $N-1$ resolution levels of wavelet coefficients (*HF coefficients*) and a coarsest level (*LF coefficients*). These coefficients are *tridimensional* vectors $(x_{i,1}\ x_{i,2}\ x_{i,3})$, where i stands for the resolution index. In our work, we choose the Loop DWT because this transform gives good visual results in 3D meshes compression [3]. Then, we use an optimal nearly uniform scalar quantizer with non uniform quantization step as described in [7]. The quantized wavelet coefficients are entropy coded using EBCOT coder [11, 6]. This lossless context based coder, included in JPEG 2000 [12], creates an embedded bitstream. Zerotree coding as SPIHT [8] could also be a good candidate [3]. However, EBCOT coder has been shown more efficient for images than SPIHT [12].

3. Wavelet coefficients model

3.1 Correlation of wavelet vectors

Table 1 shows the normalized zero-mean cross-correlations $\rho\{x_{i,1}, x_{i,2}\}$, $\rho\{x_{i,1}, x_{i,3}\}$ and $\rho\{x_{i,2}, x_{i,3}\}$

*This work is supported by a grant from the region PACA and Opteway Corporation in Sophia Antipolis, France.

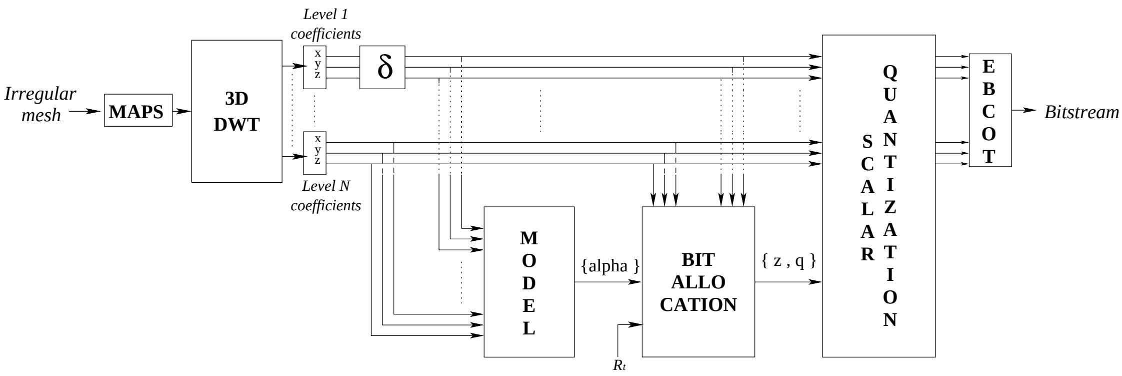

Figure 1. Proposed geometry compression scheme.

level	$\rho\{x_{i,1}, x_{i,2}\}$	$\rho\{x_{i,1}, x_{i,3}\}$	$\rho\{x_{i,2}, x_{i,3}\}$
1 (finest)	0.063	-0.003	0.093
2	0.040	0.002	-0.006
3	0.114	0.037	0.045
4	0.152	-0.017	-0.036
5	0.299	0.077	0.008
coarsest	-0.331	-0.252	0.436

Table 1. Correlation between coordinates.

between the different coordinates of each resolution level, computed for the 3D object *horse*. Typically, we observe that most of computed coefficients are located around zero, showing that coordinates present low correlation. By this way, we propose a separate quantization process for each HF coordinate $\{x_{i,j}\}$. On the other hand, LF coefficients are correlated, and cannot be processed like HF ones (see Section 4.1).

3.2 Wavelet coefficients distribution

The only way to allocate the bitrates in the different subbands without pre-quantizing each subband is to perform a model-based bit allocation, depending on distortion and rate models, and the wavelet coefficients distributions. In this paper, we focus on the modeling of the particular distribution of these coefficients. Figure 2 shows three typical probability density functions (pdf) with respect to the x axis, for the finer resolution level and two other resolutions. We can observe that all HF subband distributions are zero mean and all informations are concentrated on few coefficients (very small variances). It can be shown that a good approximation for each HF coordinate pdf is given by the *generalized Gaussian distribution* [1]:

$$p(x) = ae^{-|bx|^{\alpha}} \quad (1)$$

with $b = \frac{1}{\sigma}\sqrt{\frac{\Gamma(3/\alpha)}{\Gamma(1/\alpha)}}$ and $a = \frac{b\alpha}{2\Gamma(1/\alpha)}$. The parameter α is computed using the variance and the fourth-order moment of each subband $\{x_{i,j}\}$.

3.3 Rate and distortion models

For each coordinate subband $\{x_{i,j}\}$, the bitrate $R_{i,j}$ related to a deadzone scalar quantizer $\{q_{i,j}, z_{i,j}\}$, is estimated by computing the entropy:

$$R_{i,j} = -\sum_{m_{i,j}=-\infty}^{+\infty} Pr(m_{i,j})\ log_2\ Pr(m_{i,j}) \quad (2)$$

with $Pr(m_{i,j})$ the probability of a quantization level $m_{i,j}$:

$$Pr(m_{i,j}) = \int_{\frac{z_{i,j}}{2}+|m_{i,j}|q_{i,j}}^{\frac{z_{i,j}}{2}+(|m_{i,j}|-1)q_{i,j}} p(x_{i,j})dx_{i,j} \quad (3)$$

$$\text{and } Pr(0) = \int_{-\frac{z_{i,j}}{2}}^{+\frac{z_{i,j}}{2}} p(x_{i,j})dx_{i,j} \quad (4)$$

Furthermore, the related model-based distortion $\sigma^2_{Q_{i,j}}$ for the i, jth subband is:

$$\sigma^2_{Q_{i,j}} = \int_{-\frac{z_{i,j}}{2}}^{+\frac{z_{i,j}}{2}} p(x_{i,j})dx_{i,j} + 2\sum_{m_{i,j}=1}^{+\infty} \int_{\frac{z_{i,j}}{2}+|m_{i,j}|q_{i,j}}^{\frac{z_{i,j}}{2}+(|m_{i,j}|-1)q_{i,j}} (x_{i,j}-\hat{x}_{i,j})^2 p(x_{i,j})dx_{i,j} \quad (5)$$

where $x_{i,j}$ is an original sample and $\hat{x}_{i,j}$ its corresponding quantization sample. For a generalized Gaussian distribution, formula (5) can be written as:

$$\sigma^2_{Q_{i,j}} = \sigma^2_{i,j} D_{i,j}\left(\frac{z_{i,j}}{\sigma_{i,j}}, \frac{q_{i,j}}{\sigma_{i,j}}\right) \quad (6)$$

with $\sigma^2_{i,j}$ the variance of subband i, j. See [6, 7] for more explanations.

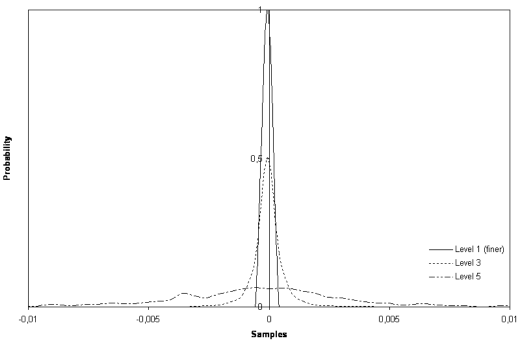

Figure 2. Coefficients distributions

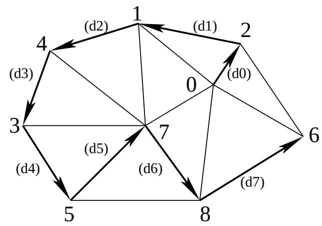

Old indices	0	2	1	4	3	5	7	8	6
New indices	0	1	2	3	4	5	6	7	8

Figure 3. Predictive coding of LF coefficients.

4 Geometry coding

4.1 Predictive coding for LF coefficients

It can be shown that LF coefficients present high correlation with respect to their 1-neighborhood v_1 (see table 2). In order to take into account this correlation, we use a predictive method and propose to model the *differences* between two LF coefficients instead of the LF vectors themselves. Indeed, these difference vectors present low cross-correlation (see table 2): each coordinate can then be processed separately. Moreover, they can be modeled by a generalized Gaussian distribution.

Let $X_{LF} = \{X_i, for\ all\ i \in [0, \#LFvertices]\}$ be the set of LF vectors, let δ be the output set of difference vectors and I the output set of new-ordered indices. The pseudo-code is:

1. The first reference vector X is X_0; $I = \{0\}$; X_{LF} contains all LF vectors excepted X_0;
2. Find X_i the closest point of X among X_{LF} by minimizing $||X - X_i||^2$;
3. Add i in I and the difference vector $(X - X_i)$ in δ;
4. Remove X_i from X_{LF}; $X \leftarrow X_i$;
5. If X_{LF} is not empty, return to step 2 else stop.

The obtained set δ represents the three *LF subbands* and will be considered by the allocation process like classical wavelet coefficients (see section 4.2). On the other hand, the set I must be known by decoder since the order of δ is different of the original list of vectors.

$\rho\{x_{1,1}, v_1(x_{1,1})\}$	$\rho\{x_{1,2}, v_1(x_{1,2})\}$	$\rho\{x_{1,3}, v_1(x_{1,3})\}$
0.862	0.979	0.978
$\rho\{\delta x_{i,1}, \delta x_{i,2}\}$	$\rho\{\delta x_{1,1}, \delta x_{1,3}\}$	$\rho\{\delta x_{1,2}, \delta x_{1,3}\}$
-0.04	0.07	0.280

Table 2. Correlation of LF difference vectors.

In order to avoid an additionnal binary cost by transmitting I, we adjust at coding step the order of LF coefficients to one which is given by I (see figure 3: example with 9 vertices indexed from 0 to 8. The arrows show the predicted path found by the algorithm).

4.2 Optimal Bit allocation

This is the crucial step of our compression scheme. The main idea is to determine the best set of deadzones and quantization steps $\{z_{i,j}, q_{i,j}\}$ for each subband (in our case, sets of coordinates $\{x_{i,j}\}$ for i and j fixed) that minimizes the distortion $\sigma^2_{Q_{i,j}}$ at a given rate [7].

By introducing Lagrangian operators, this constrained allocation problem can be written as:

$$J(\{z_{i,j}, q_{i,j}\}, \lambda) = \sum_{i=1}^{N}\sum_{j=1}^{3} \Delta_{i,j}\pi_{i,j}\sigma^2_{i,j} D_{i,j}(\frac{z_{i,j}}{\sigma_{i,j}}, \frac{q_{i,j}}{\sigma_{i,j}}) + \lambda(\sum_{i=1}^{N}\sum_{j=1}^{3} a_{i,j} R_{i,j}(\frac{z_{i,j}}{\sigma_{i,j}}, \frac{q_{i,j}}{\sigma_{i,j}}) - R_T) \quad (7)$$

where $\pi_{i,j}$ and $\Delta_{i,j}$ are optional weights respectively for taking account of the non-orthogonality of the filter bank and for frequency selection. The coefficients $a_{i,j}$ depend on the subsampling and correspond to $a_{i,j} = size(\{x_{i,j}\})/(3 \times \#$ semi-regular vertices). $D_{i,j}$ and $R_{i,j}$ depend only on α and the quotients $\frac{z_{i,j}}{\sigma_{i,j}}$ and $\frac{q_{i,j}}{\sigma_{i,j}}$.

By differentiating expression (7) with respect to $z_{i,j}$, $q_{i,j}$ and λ, and by solving the resulting system, we obtain the optimal relationships [7]:

$$h_{i,j}(\frac{q_{i,j}}{\sigma_{i,j}}) = \frac{\frac{\partial D_{i,j}}{\partial x_2}(g_i(\frac{q_{i,j}}{\sigma_{i,j}}), \frac{q_{i,j}}{\sigma_{i,j}})}{\frac{\partial R_{i,j}}{\partial x_2}(g_i(\frac{q_{i,j}}{\sigma_{i,j}}), \frac{q_{i,j}}{\sigma_{i,j}})} = -\lambda \frac{a_{i,j}}{\Delta_{i,j}\pi_{i,j}\sigma^2_{i,j}} \quad (8)$$

$$\sum_{i=1}^{N}\sum_{j=1}^{3} a_{i,j} R_{i,j}(g_{i,j}(\frac{q_{i,j}}{\sigma_{i,j}}), \frac{q_{i,j}}{\sigma_{i,j}}) - R_T = 0 \quad (9)$$

with $\frac{z_{i,j}}{\sigma_{i,j}} = g_{i,j}(\frac{q_{i,j}}{\sigma_{i,j}})$ for a given λ. $h_{i,j}$ is used in (8) to simplify the notations.

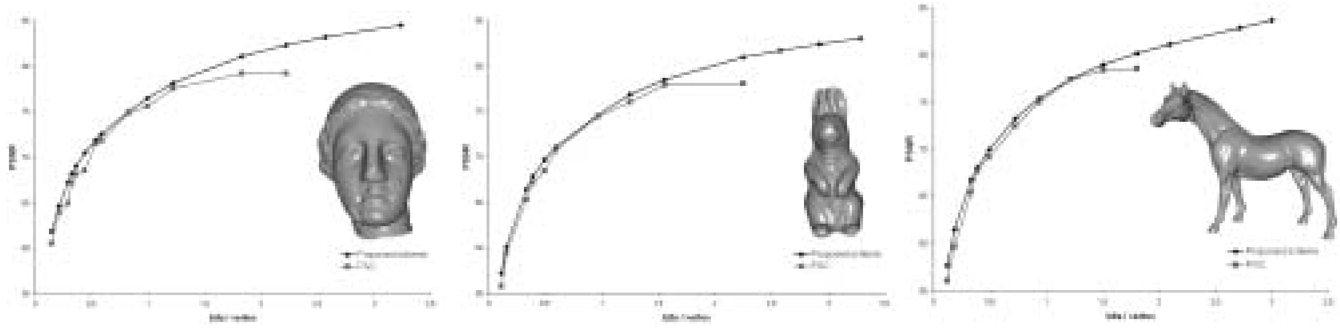

Figure 4. Geometry coding: PSNR (on semi-regular mesh) vs Rate for venus, rabbit and horse objects.

This allocation needs three functions depending on the distribution model: $ln(-h_{i,j}) = f_1(R_{i,j})$, $R_{i,j} = f_2(\frac{q_{i,j}}{\sigma_{i,j}})$ and $\frac{z_{i,j}}{\sigma_{i,j}} = g_{i,j}(\frac{q_{i,j}}{\sigma_{i,j}})$. For low complexity purposes, we use pre-computed tables.

The bit allocation algorithm is the following:

1. λ is given. Compute $-\lambda\frac{a_{i,j}}{\Delta_{i,j}\pi_{i,j}\sigma^2_{i,j}} = ln(-h_{i,j})$ and read the resulting bitrate $R_{i,j}$ from the first pre-computed tables.
2. While (9) is not verified (below a given threshold), calculate a new λ by dichotomy and return to step 1;
3. Compute $\frac{q_{i,j}}{\sigma_{i,j}}$ for each subband using the tabulated function $R_{i,j} = f_2(\frac{q_{i,j}}{\sigma_{i,j}})$;
4. Use the table $\frac{z_{i,j}}{\sigma_{i,j}} = g_{i,j}(\frac{q_{i,j}}{\sigma_{i,j}})$ to find $z_{i,j}$.

During bit allocation, the convergence is found after few iterations. Finally, subbands are quantized using the optimal set $\{z_{i,j}, q_{i,j}\}$ and encoded with EBCOT.

5 Experimental results

Our geometry coder is compared with the PGC method one [3]. The comparison criteria are: the bitrates (bits/vertex) with respect to the number of vertices of the semi-regular mesh and the Peak SNR: $PSNR = 20log_{10}(peak/d)$, with $peak$ the bounding box diagonal and d the RMSE between original semi-regular mesh and quantized one. Figures 4 show results for the 3D objects *venus*, *rabbit* and *horse*. We can observe the efficiency of the proposed bit allocation: our results are similar or superior to those obtained by PGC method for these three objects.

6 Conclusions

In this paper, we proposed a new compression scheme using model-based geometry coding of 3D wavelet coefficients. The efficiency of this coder comes from the bit allocation: bits are dispatched across subbands according to their variance. Moreover, the original predictive coding method for LF coefficients permit a modelisation of LF subbands despite the non particular statistical distributions. It provides results slighly better than PGC method [3].

References

[1] M. Antonini, M. Barlaud, P. Mathieu, and I. Daubechies. Image coding using wavelet transform. *IEEE Trans. on IP*, April 1992.

[2] M. Deering. Geometry compression. *SIGGRAPH*, 1995.

[3] A. Khodakvosky, P. Schroder, and W. Sweldens. Progressive geometry compression. *SIGGRAPH*, 2000.

[4] A. Lee, W. Sweldens, P. Schroder, P. Cowsar, and D. Dobkin. MAPS: Multiresolution adaptive parametrization of surfaces. *SIGGRAPH*, 1998.

[5] M. Lounsbery, T. DeRose, and J. Warren. Multiresolution analysis for surfaces of arbitrary topological type. *Trans. on Graphics 16,1*, 99, 1997.

[6] C. Parisot, M. Antonini, and M. Barlaud. Model-based bit allocation for jpeg2000. *Proc. of EUSIPCO*, september 2002.

[7] C. Parisot, M. Antonini, and M. Barlaud. Optimal nearly uniform scalar quantizer design for wavelet coding. *Proc. of SPIE VCIP Conference*, january 2002.

[8] A. Said and W. Pearlman. A new and efficient image codec based on set partitioning in hierarchical trees. *IEEE Trans. on CSVT*, 6, june 1992.

[9] G. Taubin and J. Rossignac. Geometric compression through topological surgery. *ACM Trans. on Graphics*, April 1998.

[10] G. Taubin and J. Rossignac. 3D geometry compression. *Course notes No 21, ACM SIGGRAPH 99*, 1999.

[11] D. Taubman. High performance scalable image compression with EBCOT. *submitted to IEEE Trans. on IP*, August 1999.

[12] I. J. WG1. Jpeg2000 part 1 final draft international standard. *http://www.jpeg.org.*